Canadian Journal of
Forest Research

Research Article

A method for updating variable radius plot surveys

Bryce Frank[a], **Francisco Mauro**[b], **Constance A. Harrington**[a], **and Kevin R. Ford**[c]

[a]USDA Forest Service, Pacific Northwest Research Station, 3625 93rd Avenue SW, Olympia, WA 98512, US; [b]iuFOR, EiFAB, University of Valladolid, E- 42004 Soria, Spain; [c]USDA Forest Service, Pacific Northwest Region, 1220 SW 3rd Avenue, Portland, OR 97204, US

Corresponding author: **Bryce Frank** (email: bryce.frank@usda.gov)

Abstract

Variable radius plot surveys can require updated estimates when the quality of previous estimates have declined over time. We developed a statistical estimator for this purpose that is the product of two estimators, one estimator is for the updated volume-to-basal-area ratio and the other estimator is for the updated basal area. Our estimator relies only on the surveyor identifying previously measured trees and does not require the identification of ingrowth, which simplifies its application. We also propose a variance estimator that relies on the bootstrap method. We investigate the point and variance estimators under repeated sampling of stem-mapped populations that include five measurements over a period of approximately 20 years. Based on 144 sampling scenarios, our estimator demonstrated relative biases ranging between −0.3% and 0.8%. The bootstrap variance estimator tended to be deflated, with relative absolute biases ranging between −8% and 4%. When revisiting one third of the initially installed plots, our estimator obtained relative root mean square errors within 1.6% of an independent resurvey effort that does not use the prior survey. This implies that our estimator can substantially reduce field work while producing surveys of approximately the same quality when updating prior surveys.

Key words: variable radius plots, double sampling, bootstrap variance estimation, product estimator, sampling designs

1. Introduction

Variable radius plot (VRP) surveys are frequently used by forest managers to assess the current state of forest stands. VRP surveys are lauded for their efficiency when estimating variables of interest that are correlated with basal area, and as such are a mainstay in forest inventory operations across the world. A rich history of methodological development has spurred the ubiquity of VRP surveys, spanning decades, with developments primarily concentrated toward the objective of estimating standard timber volume and value (Bitterlich 1984). In the modern day, VRP surveys can be used for a vast array of quantities of interest ranging from merchantable timber volume (Hamilton et al. 1999), aboveground biomass (Ducey 2009), and the estimation of forest growth components (Scott 1990; Stewart 2007).

In some cases, the information from an initial VRP survey may not be suitable for making current forest management decisions. For example, a planned forest management action for a stand or project area with a VRP survey may be delayed for operational reasons such as contract delays, market fluctuations, or re-orientation of management objectives by a forest management agency or company, motivating an updated survey at a later date. In other cases, frequent inventory updates may be necessary to satisfy internal or external requirements, as in the case of some voluntary carbon market methodologies (e.g., American Carbon Registry 2021). In these cases, forest management organizations may be tasked with efficiently updating prior surveys to ensure estimates are rigorous and defensible. We use the term "update" to refer to the task of adjusting estimates from the previous VRP survey, which may not reflect current conditions, to reflect the current state of the stand or project area.

An open question is how a forest management agency might conduct an update to a prior VRP survey. This study develops an estimator for this purpose that uses ideas from double sampling. Double sampling contains a broad family of approaches that collect a large initial sample of a covariate that is anticipated to be correlated with a variable of interest. A subsample is collected to obtain observations of the variable of interest and a covariate together for a subset of the initially sampled elements (e.g., Särndal et al. 2003, pp. 343–345). Then, an estimator is constructed that leverages the correlation between the covariate and the variable of interest, which may improve the precision of estimates of totals and means for a population (Wilm et al. 1944; Dellenbaugh et al. 2007). Double sampling is widely used in many fields, and it has a rich history of application in forest inventories (Williams 2001; Dahl et al. 2008; Hsu et al. 2020).

Developing an estimator that updates a prior VRP survey is the primary objective of this study. We propose an estimator that is composed of the product of two estimators, one for the volume-to-basal-area ratio (VBAR) and one for basal area at the revisit date, which we call the product update estimator (PUE). The estimate for the basal area is updated using a traditional double sampling estimator, and the estimate for the volume-to-basal-area is updated using a double sampling estimator that is extended to consider ingrowth trees. Additionally, we develop a bootstrap estimator for the variance of the PUE. Following this, we examine the behavior of the PUE and its variance estimator using a Monte Carlo simulation of two repeatedly measured stem mapped stands located on the Olympic Peninsula in western Washington. The stands contain approximately 20 years of remeasurement, with measurement intervals spanning 5 years, which enables an in-depth analysis of the temporal aspects of the PUE on real populations of trees. We conclude with suggestions for practical implementation of the PUE and opportunities for further research. Additionally, an implementation of the PUE and its variance estimator in R are provided as supplemental material.

2. Materials and methods

2.1. Variable radius plot updates

Many possible sampling designs can be considered when developing estimators that update a prior VRP survey. In this section, we outline a general framework for composing a VRP survey at the first visit, referred to as $t = 1$, with an associated update survey at the second visit, referred to as $t = 2$. Specifically, we assume that a set of sample locations at $t = 1$ was collected using a uniform intensity probability design, such as systematic random sampling or simple random sampling. Let the set $\mathcal{I}_1 = \{i : i = 1, \ldots, n_1\}$ refer to the set of plot indices at $t = 1$, where n_1 is the number of plots collected at $t = 1$. Note that $\mathcal{I}$ is a scripted letter "I". At each plot, trees are tallied with a prism (or similar tool) using a fixed basal area factor (BAF). Let $\mathcal{T}_1 = \{\mathcal{T}_{1i} : i \in \mathcal{I}_1\}$ refer to a set of sets indexing the tally trees at $t = 1$, i.e., $\mathcal{T}_{1i}$ is the set of tally trees on plot i. Let $\dot{\mathcal{T}}_1 = \left\{\dot{\mathcal{T}}_{1i} : i \in \mathcal{I}_1\right\}$ refer to a set of sets containing measure trees, where $\dot{\mathcal{T}}_{1i} \in \mathcal{T}_{1i}$ refers to a plot-level set of the measure trees obtained at $t = 1$. We assume in this study that only those trees that meet a pre-determined merchantability standard are tallied, and thus are eligible for measurement. For our purposes, we define the merchantability standard as live trees with diameter at breast height of at least 12 cm that are free of defect, but other standards could be applied.

With the first survey established, we assume that at $t = 2$ a subset of the sample plots from $t = 1$ are reselected using simple random sampling without replacement and trees are selected into the sample of tally trees using the same BAF. We obtain the $t = 2$ tally sets $\mathcal{T}_2 = \{\mathcal{T}_{2i} : i \in \mathcal{I}_2\}$, where $\mathcal{I}_2$ is a set indexing the revisited plots, of size n_2. Note that $n_2 \leq n_1$ under this design. Let $\dot{\mathcal{T}}_2 = \left\{\dot{\mathcal{T}}_{2i} : i \in \mathcal{I}_2\right\}$, where $\dot{\mathcal{T}}_{2i}$ refers to the set of measure trees obtained from plot i at $t = 2$. Specifying a revisited VRP survey in this way allows for explicit summations over sets of trees that form the estimators we introduce in the following sections.

We propose a method of selecting measure trees at $t = 2$ that requires the surveyor to identify two distinct sets of tally trees. We first define a set that refers to the tallied trees at $t = 2$ that were not measured at $t = 1$ using the set notation $\mathcal{A}_{2i}$, which can be thought of as a set of "additional trees". This set of trees may include (1) ingrowth trees, (2) merchantable trees that were only tallied at $t = 1$ but not measured, and (3) merchantable trees at $t = 1$ that grew of sufficient size to intersect the VRP sample plot at $t = 2$, also referred to as on-growth trees, e.g., Scott (1990). The determination of the set $\mathcal{A}_{2i}$ requires only two tasks in the field. First, the surveyor tallies the trees, then they determine which of the tally trees were not measured at $t = 1$ (or, conversely, the surveyor identifies which trees were measured at $t = 1$). We proceed under the assumption that this determination is feasible, e.g., by using data records from the previous survey or permanent tree tags and markings, and include some discussion toward violations of this assumption in the "Discussion" section. The second set is the previously measured trees that are also tallied at $t = 2$, which is the set $\dot{\mathcal{T}}_{1i}$ defined previously.

We consider the specific case of Bernoulli sampling to collect measure trees at each visit. At $t = 1$, trees within each tally set $\mathcal{T}_{1i}$ are selected for measurement with probability of success defined as $p_{\dot{\mathcal{T}}_1}$, forming the set $\dot{\mathcal{T}}_{1i}$. Note that by setting $p_{\dot{\mathcal{T}}_1} = 1$, we obtain the specific case where every tally tree is measured at $t = 1$. Each measurement must consist of an attribute of interest v_{ijt} (e.g., volume) and the basal area g_{ijt}, where i indexes the plot, j indexes the tree, and t indexes the time or survey visit. Bernoulli sampling is commonly conducted on federal forest lands (USDA Forest Service 1993, p. 180). Other strategies of subsampling, such as the "big BAF" method (Marshall et al. 2004) or the "point count/measure plot" method (USDA Forest Service 1993, p. 172) may be compatible with our methods with some further investigation. However, we do not consider these subsampling alternatives in the interest of limiting the scope of the study. At $t = 2$, we require the surveyor to subsample measure trees over two sets. The first set is the set of trees previously measured, $\dot{\mathcal{T}}_{1i}$, and the second set is the set of additional trees, $\mathcal{A}_{2i}$. Trees from $\dot{\mathcal{T}}_{1i}$ are selected for remeasurement with probability $p_{\ddot{\mathcal{T}}_1}$ and trees from $\mathcal{A}_{2i}$ are selected for measurement with probability $p_{\dot{\mathcal{A}}_2}$. Note that the probabilities $p_{\dot{\mathcal{T}}_1}$, $p_{\ddot{\mathcal{T}}_1}$ and $p_{\dot{\mathcal{A}}_2}$ are determined by the surveyor, and we provide some guidance for selecting feasible probabilities in Appendix A. We refer to the measure tree sets collected at $t = 2$ as $\ddot{\mathcal{T}}_{1i}$ and $\dot{\mathcal{A}}_{2i}$, respectively. Finally, we reserve the nonscripted capital letters of each set to refer to the number of trees in these sets. For example, $\dot{T}_{2i}$ and T_1 refer to the number of trees in $\dot{\mathcal{T}}_{2i}$ and $\mathcal{T}_1$, respectively. Table 1 provides a summary of the sets used to define tally trees and measure trees. Figure 1 displays the sets obtained when revisiting a plot.

2.2. Product update estimator (PUE)

The PUE for volume is

$$\widehat{V}_{2,\mathrm{PUE}} = \widehat{R}_{2,\mathrm{UE}} \cdot \widehat{G}_{2,\mathrm{UE}} \tag{1}$$

where $\widehat{R}_{2,\mathrm{UE}}$ is an estimator for the VBAR at $t = 2$ and $\widehat{G}_{2,\mathrm{UE}}$ is an estimator for the basal area per hectare at $t = 2$. While we use volume as an example of a variable of interest throughout the paper, these methods can be easily applied to other important variables such as biomass and carbon. This estimator has a natural appeal, because the functional form matches that of the so-called product estimator commonly used in

Table 1. Description of plot-level set and size notation used to construct the product update estimator.

Set type	Set notation	Set size notation	Description
Tally tree	$\mathcal{T}_{1i}$	T_{1i}	The set of tally trees on plot i at $t = 1$.
	$\mathcal{T}_{2i}$	T_{2i}	The set of tally trees on plot i at $t = 2$.
	$\mathcal{A}_{2i}$	A_{2i}	The set of tally trees on plot i at $t = 2$ that were not measured at $t = 1$. Referred to as "additional trees".
Measure tree	$\dot{\mathcal{T}}_{1i}$	$\dot{T}_{1i}$	The set of measure trees selected from $\mathcal{T}_{1i}$, measured at $t = 1$.
	$\ddot{\mathcal{T}}_{1i}$	$\ddot{T}_{1i}$	The set of measure trees selected from $\dot{\mathcal{T}}_{1i}$, measured at $t = 2$.
	$\dot{\mathcal{A}}_{2i}$	$\dot{A}_{1i}$	The set of measure trees selected from $\mathcal{A}_{2i}$, measured at $t = 2$.
	$\dot{\mathcal{T}}_{2i}$	$\dot{T}_{2i}$	The set of measure trees measured at $t = 2$, $\dot{\mathcal{T}}_{2i} = \ddot{\mathcal{T}}_{1i} \cup \dot{\mathcal{A}}_{2i}$.

Note: The set size notation refers to the number of trees within the set.

Fig. 1. A visual description of the sets of trees in a hypothetical variable radius plot at two different time points. The black X represents the plot center. Circles with a solid outline indicate tally trees, and circles with a dotted outline are trees that are not tallied. Circles colored light gray indicate trees that are selected for measurement at time t, and dark gray circles indicate trees that are remeasured at $t = 2$. Applying the set notation, we obtain $\mathcal{T}_{1i} = \{1, 5\}$, $\dot{\mathcal{T}}_{1i} = \{1\}$, $\mathcal{T}_{2i} = \{1, 3, 4, 5, 6\}$, $\ddot{\mathcal{T}}_{1i} = \{1\}$, $\mathcal{A}_{2i} = \{3, 4, 5, 6\}$, and $\dot{\mathcal{A}}_{2i} = \{4, 5\}$.

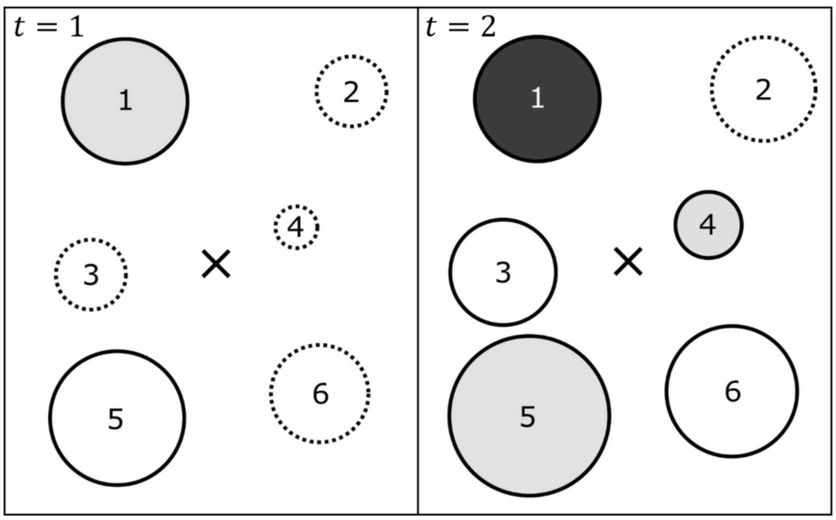

VRP surveys (Iles 2012), also referred to as the "VBAR method" (Van Deusen and Meerschaert 1986). However, the estimators we propose for R and G are ratio estimators that leverage information from $t = 1$, rather than using information solely from revisited plots. We refer to this estimator as the PUE. Expanding the right-hand-side we obtain

$$(2) \qquad \widehat{V}_{2,\mathrm{PUE}} = \left[\widehat{R}'_1 \cdot \frac{\widehat{R}_2}{\widehat{R}_1}\right] \cdot \left[\widehat{G}'_1 \cdot \frac{\widehat{G}_2}{\widehat{G}_1}\right]$$

where $\widehat{R}'_1$ and $\widehat{G}'_1$ refer to the estimators of VBAR and basal area using the first survey, and are the typical estimators used in the product estimator for single date surveys. In contrast, the ratios $\frac{\widehat{R}_2}{\widehat{R}_1}$ and $\frac{\widehat{G}_2}{\widehat{G}_1}$ are constructed using only data from the revisited plots. These ratios are what allow the PUE to achieve reductions in variance relative to an estimator used without information from $t = 1$ (Cochran 1977; Reich et al. 1993).

We turn now to each component of the PUE. First, we require an estimator for the VBAR at $t = 1$ using all initially installed plots

$$(3) \qquad \widehat{R}'_1 = \frac{1}{\dot{T}_1} \sum_{\mathrm{i} \in \mathcal{I}_1} \sum_{\mathrm{j} \in \dot{\mathcal{T}}_{1\mathrm{i}}} \frac{v_{\mathrm{ij1}}}{g_{\mathrm{ij1}}}$$

Next, we require an estimator of the VBAR at $t = 1$ using only revisited plots

$$(4) \qquad \widehat{R}_1 = \frac{1}{\dot{T}_{1,\mathcal{I}_2}} \sum_{\mathrm{i} \in \mathcal{I}_2} \sum_{\mathrm{j} \in \dot{\mathcal{T}}_{1\mathrm{i}}} \frac{v_{\mathrm{ij1}}}{g_{\mathrm{ij1}}}$$

where $\dot{T}_{1,\mathcal{I}_2} = \sum_{\mathrm{i} \in \mathcal{I}_2} \dot{T}_{1\mathrm{i}}$, which represents the number of trees measured at $t = 1$ that exist on revisited plots only. Next, we require estimators for the VBAR for tree measurements obtained at $t = 2$. We produce two separate estimators, one for the set of remeasured trees, $\ddot{\mathcal{T}}_1$, and one for the set of additional measure trees, $\dot{\mathcal{A}}_2$. We obtain

$$(5) \qquad \widehat{R}_{\ddot{\mathcal{T}}_1} = \frac{1}{\ddot{T}_1} \sum_{\mathrm{i} \in \mathcal{I}_2} \sum_{\mathrm{j} \in \ddot{\mathcal{T}}_{1\mathrm{i}}} \frac{v_{\mathrm{ij2}}}{g_{\mathrm{ij2}}}$$

and

$$(6) \qquad \widehat{R}_{\dot{\mathcal{A}}_2} = \frac{1}{\dot{A}_2} \sum_{i \in \mathcal{I}_2} \sum_{j \in \dot{\mathcal{A}}_{2i}} \frac{v_{ij2}}{g_{ij2}}$$

These two estimators are combined using the weighted average

$$(7) \qquad \widehat{R}_2 = w_{\mathcal{A}_2} \widehat{R}_{\dot{\mathcal{A}}_2} + w_{\dot{\mathcal{T}}_1} \widehat{R}_{\dot{\mathcal{T}}_1}$$

where $w_{\mathcal{A}_2} = \frac{A_2}{T_2}$ is and $w_{\dot{\mathcal{T}}_1} = 1 - w_{\mathcal{A}_2}$. The weights in (7) are used to partition the two estimators of VBAR into the additional tree and remeasured tree components of the basal area. We obtain the double sampling estimator for VBAR

$$(8) \qquad \widehat{R}_{2,\mathrm{UE}} = \widehat{R}_1' \left[\frac{w_{\mathcal{A}_2} \widehat{R}_{\dot{\mathcal{A}}_2} + w_{\dot{\mathcal{T}}_1} \widehat{R}_{\dot{\mathcal{T}}_1}}{\widehat{R}_1} \right]$$

Finally, we obtain the double sampling estimator for basal area, which simplifies to

$$(9) \qquad \widehat{G}_{2,\mathrm{UE}} = \left(\frac{F}{n_1} \sum_{i=1}^{n_1} T_{1i} \right) \left(\frac{\sum_{i \in \mathcal{I}_2} T_{2i}}{\sum_{i \in \mathcal{I}_2} T_{1i}} \right)$$

where F is the BAF. Table 2 provides descriptions of each of the component estimators.

2.3. Bootstrap variance estimator

The PUE is a complex estimator involving several component estimators for R and G at different time points using different sets of trees. In light of this complexity, a route forward for variance estimation is the bootstrap method, which uses resampling methods to approximate the sampling distribution of an estimator (e.g., Shao 2003). From this distribution, we can obtain variance estimates, confidence intervals, and other quantities of interest. In the context of a VRP update as specified in this study, we require a bootstrap method that can be applied in the context of double sampling. We take inspiration from an algorithm published by Schreuder et al. (1987), who developed a bootstrap method using sampling with partial replacement, which can be viewed as a general case of double sampling.

Consider the initial sample of n_1 field plots collected by the surveyor. After the VRP update is applied, this sample can be partitioned into two components, one containing the sample plots not selected for a revisit, of size $n_1 - n_2$, and one containing the sample plots selected for revisit, of size n_2. The first partition is sampled with replacement using a sample size of $n_1 - n_2$ and the second partition is sampled with replacement using a sample size of n_2. For a given bootstrap iteration, these partitions represent a bootstrap sample of the original n_1 sample plots, of which n_2 are revisited plots. Then, bootstrap estimates of each component of the PUE can be made using the partitioned bootstrap sample. Introducing the index b to represent a bootstrap iteration, the bootstrap estimates of VBAR are $\widehat{R}_{1,b}$, $\widehat{R}'_{1,b}$, and $\widehat{R}_{2,b}$, and the bootstrap estimates of basal area are $\hat{G}_{1,b}$, $\hat{G}'_{1,b}$, and $\hat{G}_{2,b}$. A bootstrap estimate of the PUE is then given by

$$(10) \qquad \hat{V}_{\mathrm{PUE,b}} = \left[\hat{R}'_{1,b} \cdot \frac{\hat{R}_{2,b}}{\hat{R}_{1,b}} \right] \cdot \left[\hat{G}'_{1,b} \cdot \frac{\hat{G}_{2,b}}{\hat{G}_{1,b}} \right]$$

Finally, we obtain the bootstrap variance estimator

$$(11) \qquad \widehat{Var}\left(\widehat{V}_{\mathrm{PUE}}\right) = \frac{1}{B} \sum_{b=1}^{B} \left(\widehat{V}_{\mathrm{PUE,b}} - \widehat{\bar{V}}_{\mathrm{PUE}} \right)^2$$

where $\widehat{\bar{V}}_{\mathrm{PUE}} = \frac{1}{B} \sum_{b=1}^{B} \hat{V}_{\mathrm{PUE,b}}$ and the bootstrap standard error, $\widehat{SE}\left(\hat{V}_{\mathrm{PUE}}\right) = \sqrt{\widehat{Var}\left(\hat{V}_{\mathrm{PUE}}\right)}$. Further details about the bootstrap variance estimator are given in Appendix B.

To ensure convergence of the bootstrap variance estimator, we used a method that dynamically checks for convergence at each iteration of the bootstrap. This method relies on incrementing B, and stopping when a desired convergence check is met. For iterations where $B \geq 600$, we calculate the bootstrap standard error using the entire set of B bootstrap PUEs. Then, a set of preceding bootstrap standard errors are checked to see that they satisfy the stopping criterion. We obtain the stopping criterion as

$$(12) \qquad |\widehat{SE}_{\mathrm{Boot}}\left(\hat{V}_{\mathrm{PUE,B}}\right) - \widehat{SE}_{\mathrm{Boot}}\left(\hat{V}_{\mathrm{PUE,b}}\right)| \leq 0.005 \cdot \widehat{SE}_{\mathrm{Boot}}\left(\hat{V}_{\mathrm{PUE,B}}\right) \forall (B - 250) \leq b \leq (B - 1)$$

For most of the sampling scenarios, this resulted in values of B ranging between 1500 and 3000 bootstrap iterations. This procedure takes inspiration from methods proposed by Hou et al. (2019) and McRoberts et al. (2023).

2.4. Simulation study

2.4.1. Stem mapped stands

We utilized 1.44 ha stem mapped stands established in support of the Olympic Habitat Development Study (OHDS) in our simulation. These stands were established and repeatedly measured at seven locations throughout the Olympic National Forest in northwestern Washington, USA between 1996 and 2019. The stem maps were established in 30- to 70-year-old stands, primarily dominated by Douglas-fir (*Pseudotsuga menziesii* (Mirb.) Franco) and western hemlock (*Tsuga heterophylla* (Raf.) Sarg.), with smaller components of Sitka spruce (*Picea stichensis* (Bong.) Carr.), western redcedar (*Thuja plicata* Donn ex D. Don), and red alder (*Alnus rubra* Bong.). We selected the stem mapped stands from the Bait and Snow White study blocks for this study because they represented different types of post-treatment diameter distributions, with Bait containing a unimodal diameter distribution, and Snow White containing a bi-modal diameter distribution. Snow White had been commercially thinned in the 1970s, which initiated the development of a new cohort of a different species. The OHDS was established to monitor the effects of variable density thinning, which was done in 1997 and 1998

 Can. J. For. Res. 54: 1213–1229 (2024) | dx.doi.org/10.1139/cjfr-2024-0050

Table 2. Component estimators of the product update estimator.

VBAR estimators		Basal area estimators	
Estimator	Description	Estimator	Description
$\widehat{R}'_1$	An estimator for the VBAR at $t = 1$ using all initially installed plots.	$\widehat{G}'_1$	An estimator for the basal area at $t = 1$ using all initially installed plots.
$\widehat{G}'_1$	An estimator for the VBAR at $t = 1$ using only revisited plots.	$\widehat{G}_1$	An estimator for the basal area at $t = 1$ using only revisited plots.
$\widehat{R}_2$	An estimator for the VBAR at $t = 2$ using only revisited plots.	$\widehat{G}_2$	An estimator for the basal area at $t = 2$ using only revisited plots.
$\widehat{R}_{\dot{\mathcal{A}}_2}$	An estimator for the VBAR at $t = 2$ for trees not previously measured.		
$\widehat{R}_{\ddot{\mathcal{T}}_1}$	An estimator for the VBAR at $t = 2$ for previously measured trees.		

Note: VBAR, volume-to-basal-area ratio.

for Snow White and Bait, respectively. For the purposes of this study, we utilize only the post-treatment visits at each stand collected from 1999 onward, and every 5 years thereafter. Let k refer to a visit such that $k \in \{1, \ldots, 5\}$. Refer to Roberts et al. (2007) for additional information about the particular stand histories and treatments.

The stands required additional processing before they were used in the simulation study. First, to mimic a VRP survey used in support of volume yield estimation, we discarded trees that are considered nonmerchantable due to excessive damage, such as broken tops, and trees that do not meet a minimum diameter threshold of 12 cm at breast height. All records belonging to trees that experienced mortality were removed. In practice, this is equivalent to the surveyor ignoring mortality trees during the tallying process, which is common practice when assessing merchantable timber yield. Second, because the OHDS field protocol did not require height measurements for every tree, we imputed missing heights for each tree at each measurement date using a set of regional diameter-height models specific to each species in the data (Barrett 2006). We predicted merchantable tree volumes using allometric models from the National Volume Estimator Library using the measured diameters and imputed heights as inputs (Wang 2023), which are treated as the actual volumes. Figure 2 displays the stands and Fig. 3 displays the parameter values for G, R, and V at each visit. We also approximated the plot-level coefficient of variation for volume using a BAF of 4 $m^2 \cdot ha^{-1}$ and a random sample of 1000 plots, given in Fig. 3.

2.4.2. Monte Carlo simulation

The PUE point and variance estimators are evaluated using a Monte Carlo simulation. The simulation proceeds by randomly allocating VRP sample plots in each of the stands. To avoid issues involving edge effect (e.g., Flewelling and Strunk 2013), we buffered the original stand areas by 20 m on each side, which was sufficient to encompass the inclusion zones of all trees in either stand at any visit (i.e., we allowed sample plots to fall up to 20 m on each side of the stand area such that all trees of a given diameter had the same selection probability), creating a sampling region that is 2.56 ha for each stand. The values of basal area per hectare and volume per hectare are calculated by summing the values across all trees and dividing by 2.56 ha, which yields the per-hectare densities for the buffered stand. VBAR is obtained by dividing the total volume by the total basal area. Parameter values are given in Fig. 3.

In our study, the PUE is conducted by assembling pairs of visits from the selected stands, first by collecting an initial survey and then revisiting the same survey sometime later. We considered all pairs made from the first post-treatment visit and all subsequent visits, i.e., $\{1, 2\}$, $\{1, 3\}$, …, $\{1, 5\}$ for a total of four pairs for each stand. To comply with previous notation, let $t = 1$ refer to the first visit, and let $t = 2$ refer to a subsequent visit for a given pair. A random sample of n_1 plots is allocated to the buffered stand using independent draws from a bivariate uniform probability distribution. While systematic sampling is commonly used for VRP surveys, we used this design primarily to match the assumptions of the variance estimator, which allows us to estimate its bias under this "favorable" sampling design (see Section 4.2). Trees are tallied using BAF of 4 $m^2 \cdot ha^{-1}$, which was sufficient to select roughly six to nine tally trees per plot. A subset of trees is selected for measurement at $t = 1$ with probability of success $p_{\dot{\mathcal{T}}_1}$. Then, n_2 plots are revisited at $t = 2$ and trees are again selected into the sample using the same BAF. Trees are remeasured with probability $p_{\ddot{\mathcal{T}}_1}$ and new measure candidates are measured with probability $p_{\dot{\mathcal{A}}_2}$.

We developed three strategies for subsampling measure trees. These strategies are guided by the assumption that the surveyor wishes to exert no more measurement effort for each VRP plot than was done in the first survey, which aligns with the operational motivations of the PUE. For all strategies we selected an initial measurement rate, $p_{\dot{\mathcal{T}}_1}$, such that $E\left(\dot{T}_{1i}\right) = 4$, meaning four trees are initially measured at each plot, on average. Then, each strategy reduces the expected effort on the revisit from four trees, to three, and then finally two. We solve for $p_{\dot{\mathcal{T}}_1}$ using the known parameters in the stands (Fig. 3) then, for each stand visit, we set separate rates $p_{\ddot{\mathcal{T}}_1}$ and $p_{\dot{\mathcal{A}}_1}$ using an optimization routine described in Appendix A. These rates ensured that an approximately equal number of remeasure trees and additional trees are selected at each plot at $t = 2$.

Fig. 2. The Bait and Snow White stands used in the simulation study at the first visit, $k = 1$. Each point represents the location of a stem-mapped tree and are scaled proportional to basal area. The colors represent the species of the tree.

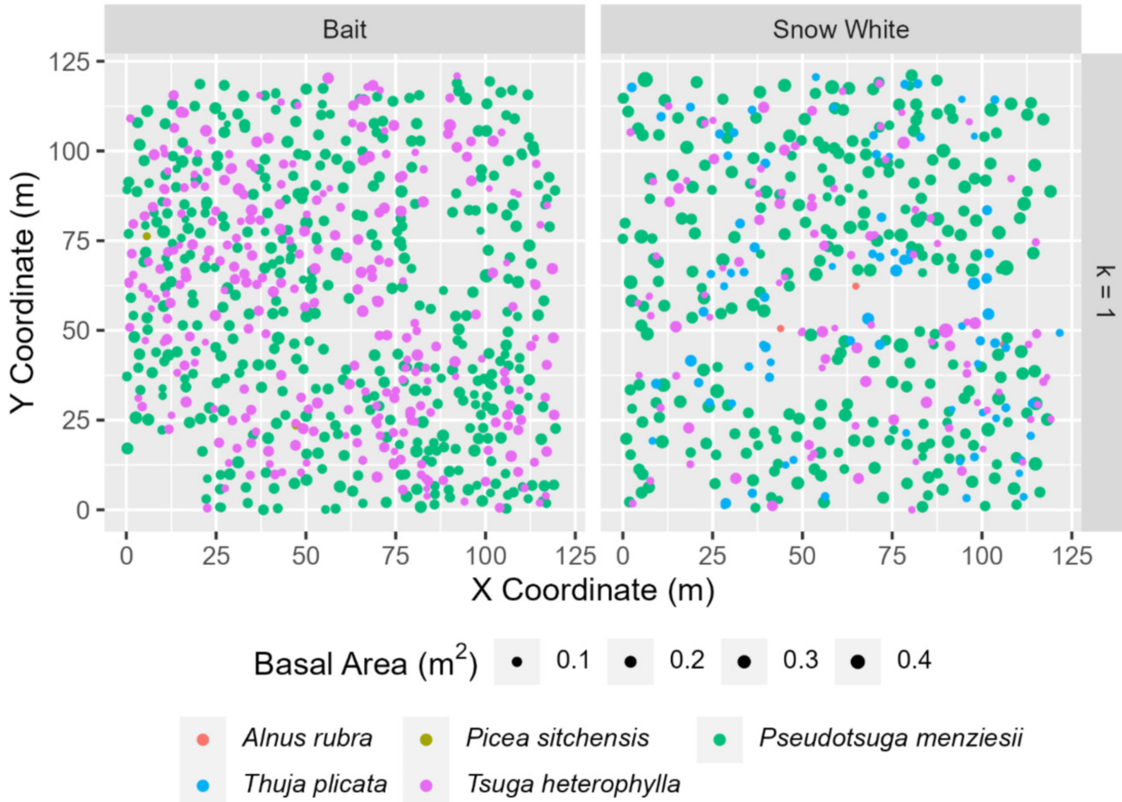

We combined the subsampling strategies with different possible sample size configurations for n_1 and n_2. For sample size n_1 we consider sample sizes of 60 and 45. For sample size n_2 we consider n_1, $n_1 \cdot \frac{2}{3}$ and $n_1 \cdot \frac{1}{3}$ as possible sample sizes, yielding six total sample size configurations. These sample size configurations are then combined with each of the three subsampling strategies, which yields 18 possible sampling designs, and are finally applied to each of the two stands containing four remeasurements for a total of 144 possible scenarios. We refer to a given sampling design by concatenating the n_1 and n_2 sample sizes with the subsampling strategy. For example, the 60–40-4 design selects 60 plots at $t = 1$, revisits 40 plots at $t = 2$, and measures approximately four trees per plot at $t = 2$.

2.4.3. Evaluation of estimators

We evaluate the PUE using various measures of performance. The approximated bias is

$$(13) \quad \mathrm{Bias}\left(\hat{V}_{2,\mathrm{PUE}}, V_2\right) = \frac{1}{M}\sum_{m=1}^{M}\hat{V}_{2,\mathrm{PUE,m}} - V_2$$

where m indexes the simulation iteration and M is the total number of iterations. We let $M = 5000$ for the remainder of the study, which was found to be sufficient for convergence of the PUE and its variance estimator using graphical inspection. We also produce the relative bias

$$(14) \quad \mathrm{Bias\%}\left(\hat{V}_{2,\mathrm{PUE}}, V_2\right) = 100 \cdot \frac{\mathrm{Bias}\left(\hat{V}_{2,\mathrm{PUE}}, V_2\right)}{V_2}$$

The approximated root mean square error (RMSE) is

$$(15) \quad \mathrm{RMSE}\left(\hat{V}_{2,\mathrm{PUE}}, V_2\right) = \sqrt{\frac{1}{M}\sum_{m=1}^{M}\left(\hat{V}_{2,\mathrm{PUE,m}} - V_2\right)^2}$$

Forest surveys are often evaluated for quality using the relative standard error (e.g., Henttonen and Kangas 2015; Yang et al. 2016). In our study, we utilize the relative RMSE, which is a more holistic measure of error when estimators are possibly biased. We obtain

$$(16) \quad \mathrm{RMSE\%}\left(\hat{V}_{2,\mathrm{PUE}}, V_2\right) = 100 \cdot \frac{\mathrm{RMSE}\left(\hat{V}_{2,\mathrm{PUE}}, V_2\right)}{V_2}$$

Note that the relative RMSE and relative standard error are equal in the case of an unbiased estimator.

In many cases, forest management organizations require VRP surveys to obtain a relative RMSE lower than some target threshold. It is reasonable to expect that these organizations would apply the same standard to VRP updates that use the

Can. J. For. Res. **54:** 1213–1229 (2024) | dx.doi.org/10.1139/cjfr-2024-0050

Fig. 3. Values of basal area per hectare (G), volume per hectare (V), volume-to-basal-area ratio (R), and the coefficient of variation for V, approximated using 1000 simulated variable radius plots and a basal area factor of 4 $m^2{\cdot}ha^{-1}$ for each stand at each visit.

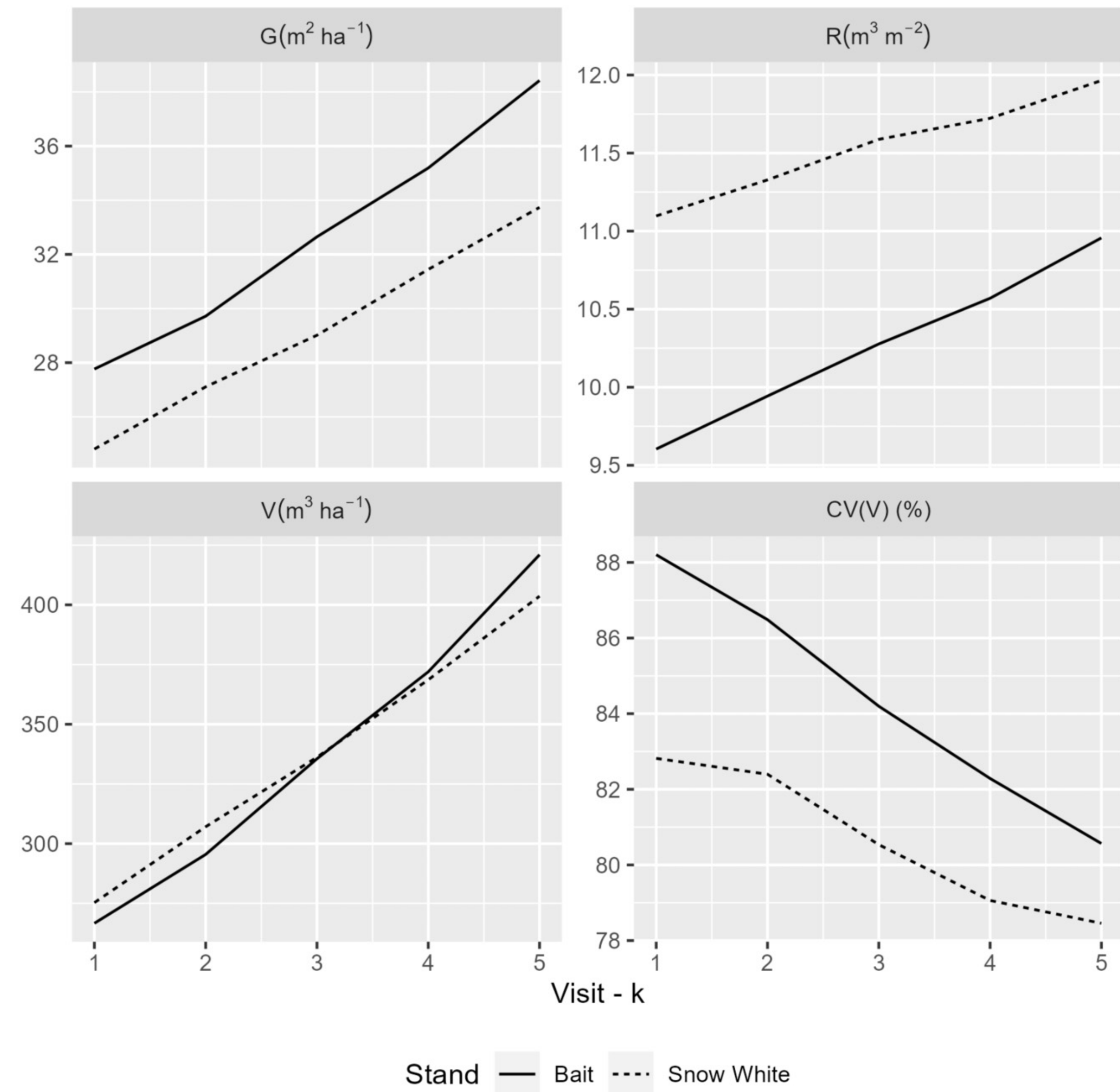

PUE. Therefore, it is of direct interest to compare the performance to the relative RMSE obtained for the first survey

$$\text{(17)} \quad \text{RMSE\%}\left(\hat{V}_1', V_1\right) = 100 \cdot \frac{\text{RMSE}\left(\hat{V}_1', V_1\right)}{V_1}$$

While we do not consider a specific error threshold in this study, we take a more conservative standpoint and examine whether the PUE achieves a lower RMSE than the first survey, assuming the first survey has met some hypothetical error threshold. We summarize the change in relative RMSE between the PUE and the first survey estimator using the difference

$$\text{(18)} \quad \text{Diff\%}\left(\hat{V}_{2,\text{PUE}}, \hat{V}_1'\right) = \text{RMSE\%}\left(\hat{V}_{2,\text{PUE}}, V_2\right) - \text{RMSE\%}\left(\hat{V}_1', V_1\right)$$

The primary motivation for using the PUE is to minimize the field work when estimating parameters of interest at $t = 2$. Therefore, it is of interest to summarize the increase or decrease in relative RMSE when adopting the PUE over the alternative approach of installing an entirely new survey. For this study, we consider the difference in relative RMSE between the PUE and an estimator made using an independently installed second survey. We obtain the difference

$$\text{(19)} \quad \text{Diff\%}\left(\hat{V}_{2,\text{PUE}}, \hat{V}_{2,n_1}\right) = \text{RMSE\%}\left(\hat{V}_{2,\text{PUE}}, V_2\right) - \text{RMSE\%}\left(\hat{V}_{2,n_1}, V_2\right)$$

where $\hat{V}_{2,n_1}$ is an estimator obtained using an independent survey collected at $t = 2$ that is composed of n_1 plots and collects approximately four measure trees per plot.

Fig. 4. Relative bias of the product update estimator (eq. 14) for each sampling design for each stand at each visit obtained from the Monte Carlo simulation. The sampling scenarios are grouped by their strategy, i.e., the approximate number of measure trees per plot selected at the revisit, and their visit, i.e., the temporal index describing the time since the initial survey. Each sampling design code on the X axis refers to the number of field plots collected at the first visit, the number of field plots collected at the second visit, and the approximate number of measure trees selected per plot at the second visit, separated by hyphens. The dashed horizontal lines indicate a relative bias threshold of +/− 1%.

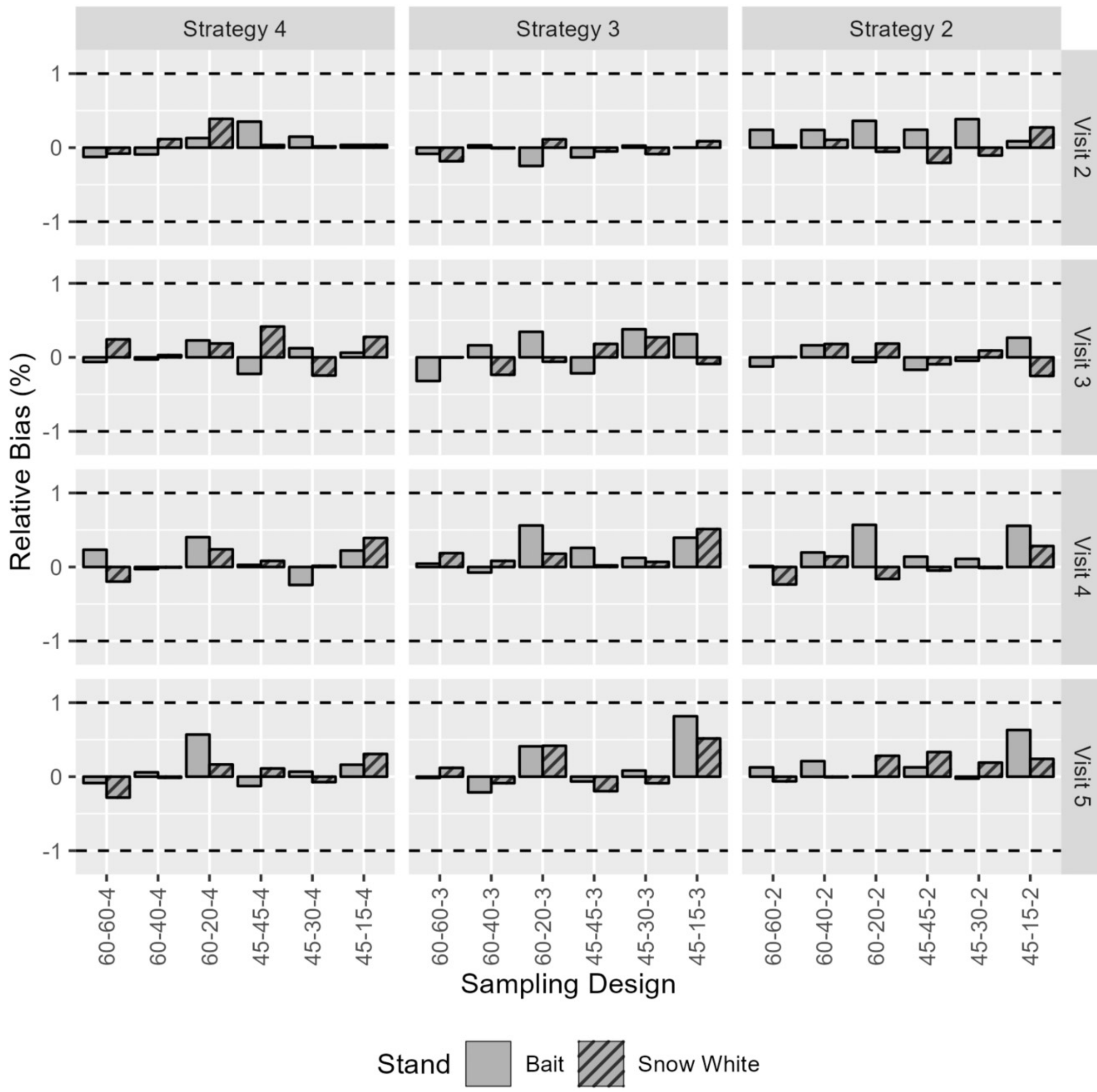

3. Results

3.1. Performance of the PUE point estimator

Following the simulation, we assess the performance of the PUE. The PUE showed relative biases ranging between −0.3% and 0.8%. Figure 4 displays the relative biases of the PUE. Across all 144 sampling scenarios, the maximum relative bias occurs in the Bait 45–15-3 scenario for the fifth visit. The bias appears to be exacerbated by smaller revisit proportion sizes, $\frac{n_2}{n_1}$, as seen in the 60–20 and 45–15 sample configurations. The bias is generally positive, but this is not uniformly the case across the sampling designs, and all relative biases fall within a +/− 1% relative bias band.

In addition to information about bias, the simulation also reveals the relative RMSE of the PUE. Overall, the relative RMSE of the PUE ranges between 9.9% and 13.8% across all simulations (Table 3). In general, the relative RMSE is primarily driven by a decreasing revisit sample fraction, $\frac{n_2}{n_1}$. For example, the largest values of relative RMSE are obtained for the 45–15-2 design, while the smallest values of relative RMSE are obtained for the 60–60-4 design in the Snow White stand. The selection of subsampling strategy for measure trees has a relatively smaller impact on the relative RMSE than the selection of the sample configuration. For example, within the Bait 60–60 sample configuration, the median relative RMSEs deviate only 0.1% from each other across strate-

Table 3. Relative root mean square errors of the product update estimator (eq. 16) for each stand and sampling design aggregated across the five visits.

Sampling design	Bait	Snow White	Sampling design	Bait	Snow White
60–60-4	10.9 (10.5–11.2)	10.2 (9.9–10.3)	45–45-4	12.7 (12.5–12.9)	11.9 (11.5–12.1)
60–60-3	10.9 (10.7–11.0)	10.2 (10.1–10.6)	45–45-3	12.6 (12.3–12.9)	11.7 (11.5–12.2)
60–60-2	11.0 (10.8–11.2)	10.4 (10.2–10.4)	45–45-2	12.8 (12.2–13.1)	11.8 (11.7–12.1)
60–40-4	11.0 (10.9–11.2)	10.3 (10.0–10.6)	45–30-4	12.8 (12.7–13.0)	12.1 (11.9–12.4)
60–40-3	11.1 (10.9–11.1)	10.4 (10.4–10.6)	45–30-3	12.9 (12.6–13.3)	12.0 (11.9–12.2)
60–40-2	11.2 (11.0–11.5)	10.5 (10.4–10.6)	45–30-2	12.7 (12.6–13.4)	12.1 (11.9–12.3)
60–20-4	11.6 (11.6–11.7)	11.0 (11.0–11.1)	45–15-4	13.5 (13.1–13.7)	12.7 (12.6–12.9)
60–20-3	11.6 (11.5–11.9)	11.0 (11.0–11.2)	45–15-3	13.5 (13.3–13.7)	12.8 (12.8–13.1)
60–20-2	11.8 (11.7–11.9)	11.2 (10.9–11.6)	45–15-2	13.7 (13.5–13.8)	12.9 (12.9–13.1)

Note: Relative root mean square error ranges across the five visits are given in parentheses below the median for each sampling design.

gies, while the median relative RMSEs moving from 60–60 to the 60–20 configuration increase by 0.7% to 0.8%. This general pattern holds across the other configurations across both stands.

The PUE is able to improve upon the precision of an estimator made during the first survey. Figure 5 displays the difference between the relative RMSE of the PUE and a relative RMSE of the estimator made at $t = 1$ (eq. 18). The 45–30 and 60–40 sample configurations are important examples of this, because they require approximately two thirds of the field effort and nearly match the precision of the first survey, which represents an important gain in reducing the field effort when adopting the PUE. Negative temporal trends are apparent in all but the 60–20 and 45–15 sample configurations, which implies that the PUE becomes more precise than the first survey over time for these designs. This is likely due to the negative trend in the coefficient of variation for volume in these stands (Fig. 3). The larger relative RMSE values for the 60–20 and 45–15 sample configurations are likely a result of the larger relative absolute biases observed in Fig. 4. As with the relative RMSEs reported in Table 3, the selection of sample strategy has a smaller impact on the difference in relative RMSEs in Fig. 5 than the sample size configuration.

The PUE can also be compared to an independent resurvey conducted at $t = 2$, which represents an alternative methodology for conducting a VRP update readily available to forest management organizations and does not require revisiting previously established plots. For this case we display the difference in relative RMSEs between the PUE and an independent resurvey in Fig. 6. The PUE tends to obtain relative RMSEs $+/-$ 0.6% from the relative RMSE of the independent resurvey when using sample configurations that revisit two thirds of the initial sample size or greater (i.e., the 60–60, 60–40, 45–45, and 45–30 configurations). This implies that, for our simulations, the PUE produces estimates of similar quality but requiring only two thirds of the initial sample size compared to an independent resurvey. For the 45–15 and 60–20 configurations, relative RMSEs increased at most 1.6%. A strong positive trend can be observed in the difference in relative RMSE% for the 60–20 and 45–15 designs, which is likely tied to the bias problems identified in Fig. 4.

3.2. Performance of the PUE variance estimator

Our simulation study enables the assessment of the bootstrap variance estimator. In general, the PUE variance estimator tends to be deflated, with relative biases ranging between -9% and 4%. Biases in the variance estimator appear to be worse when a smaller initial sample size is used (Fig. 7), or when the proportion of revisited plots is small, however, this is not uniformly the case across all scenarios. In some cases, starkly different relative biases for a given design exist when comparing between stands for some scenarios. For example, the 45–45-4 design in visit five is -6.4% for Bait, but only 0.1% for Snow White, suggesting that differences in the population of interest can drive large differences in bias in the variance estimator.

4. Discussion

4.1. Efficiency of the PUE

The PUE can establish important reductions in field work compared to an independent resurvey at $t = 2$. Our results indicated that a small increase in relative RMSE, of at most 1.6% in our simulation across a span of 20 years (Fig. 6), may occur when using PUE instead of a fully independent resurvey, specifically when the proportion of remeasured plots is reduced to one third. However, if these small losses in relative RMSE can be tolerated, important reductions in fieldwork ef-

Fig. 5. The difference between the relative root mean square error (RMSE) of the product update estimator and the relative RMSE for the first survey for each visit and sampling design (eq. 18). The values are grouped by their strategy, i.e., the approximate number of measure trees selected at each plot at the revisit, and the stand. Values above the dashed horizontal line indicate that the PUE has a larger relative RMSE than the initial survey. The line colors represent the initial sample size, n_1, and the line types represent the revisit sample proportion.

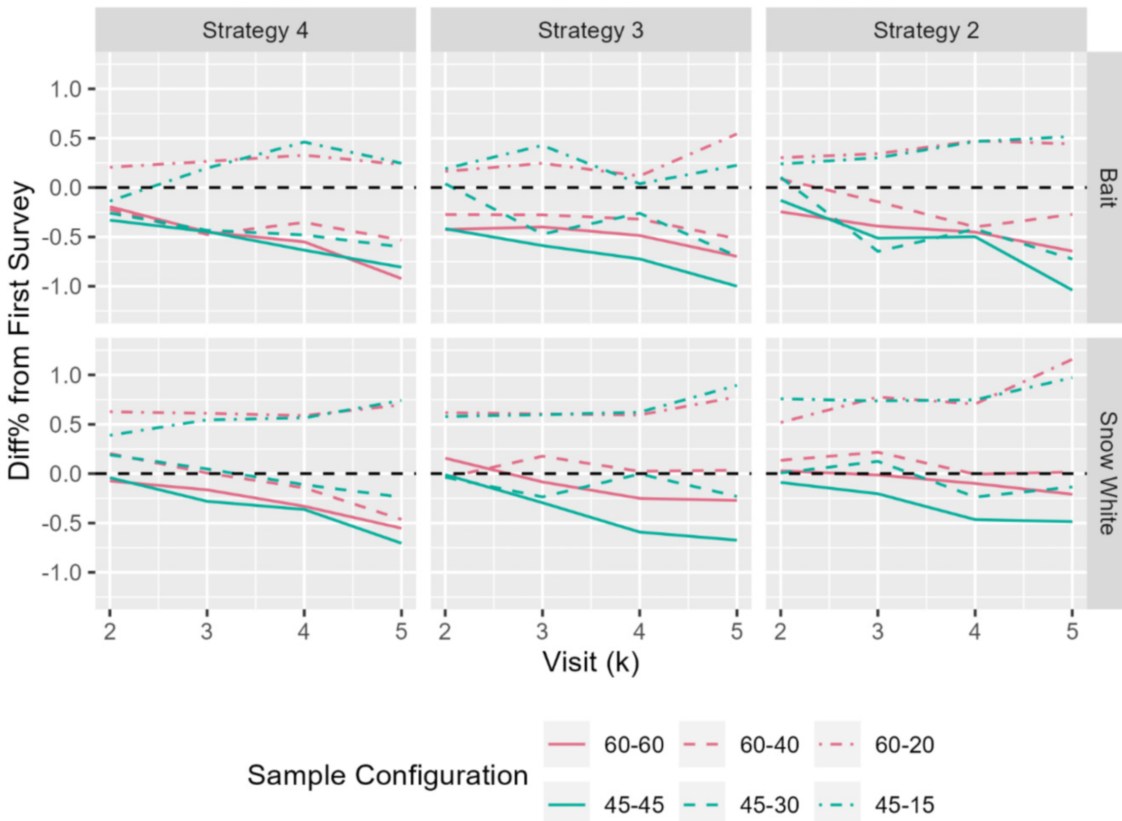

fort and cost can be achieved when applying the PUE in these contexts.

While the proportion of revisited plots is the primary driver in an increase in relative RMSE compared to a resurvey, impacts of subsampling strategies for measure trees were relatively minor. Note that our designs begin with relatively large sample sizes for VBAR trees of approximately 240 and 180 trees when $n_1 = 60$ and $n_2 = 45$, respectively. When the initial sampling variability of VBAR is small, then it may be sensible to partition a larger amount of the fieldwork effort toward retallying all plots and reducing the tree measurement effort, which corresponds to our 45–45-2 and 60–60-2 designs. These designs both achieved very similar relative RMSEs compared to Strategy 4 (Table 3), while minimizing reducing the number of collected measure trees, implying that very little precision is lost when measuring only half the amount of VBAR trees at $t = 2$.

We highlight that our approach in this study was to (1) strictly revisit previously installed plots and (2) to ensure that the effort at the second visit, measured by the number of measure trees collected per plot, did not exceed that of the first survey (Appendix A). This approach ensured that the application of the PUE for VRP survey updates was operationally simple and convenient for practitioners. However, we recognize that this is one approach of many that can help inform how to efficiently construct a sampling design for a second survey. For example, it could be possible that partitioning n_2 into plot revisits and new additional plots is more efficient for the purposes of updating a prior survey, mimicking strategies used in sampling with partial replacement (Scott and Köhl 1994). Furthermore, it may be possible to optimize the balance of the number of trees measured per plot versus the number of tally plots at the second visit analogous to prior work for single date VRP surveys (e.g., Marshall et al. 2004). Such an optimization approach could consider aspects of inter-plot travel cost versus tree-level measurement costs.

We observed that the PUE produces surveys with relative RMSEs similar to the first survey, which is an important standard to meet when the initial survey meets a pre-established maximum error threshold. Using sample configurations that revisit as little as one third of the initial plots, we observed differences in relative RMSE of at most 1.2%, while revisiting two thirds of the initial plots produced relative RMSEs that closely approach the relative RMSE of the first survey in all cases. However, we want to highlight that this behavior of the PUE will depend on the temporal dynamics of the stands under consideration. For our study, the Bait and Snow White

 Can. J. For. Res. **54:** 1213–1229 (2024) | dx.doi.org/10.1139/cjfr-2024-0050

Fig. 6. Differences in the relative root mean square error (RMSE) between the product update estimator (PUE) and the relative RMSE of the independent resurvey estimator (eq. 19). The values are grouped by their strategy, i.e., the approximate number of measure trees selected at each plot at the revisit, and the stand. Lines that fall above the horizontal dashed line represent an increase in relative RMSE when adopting the PUE instead of the independent resurvey. The line colors represent the initial sample size, n_1, and the line types represent the revisit sample proportion.

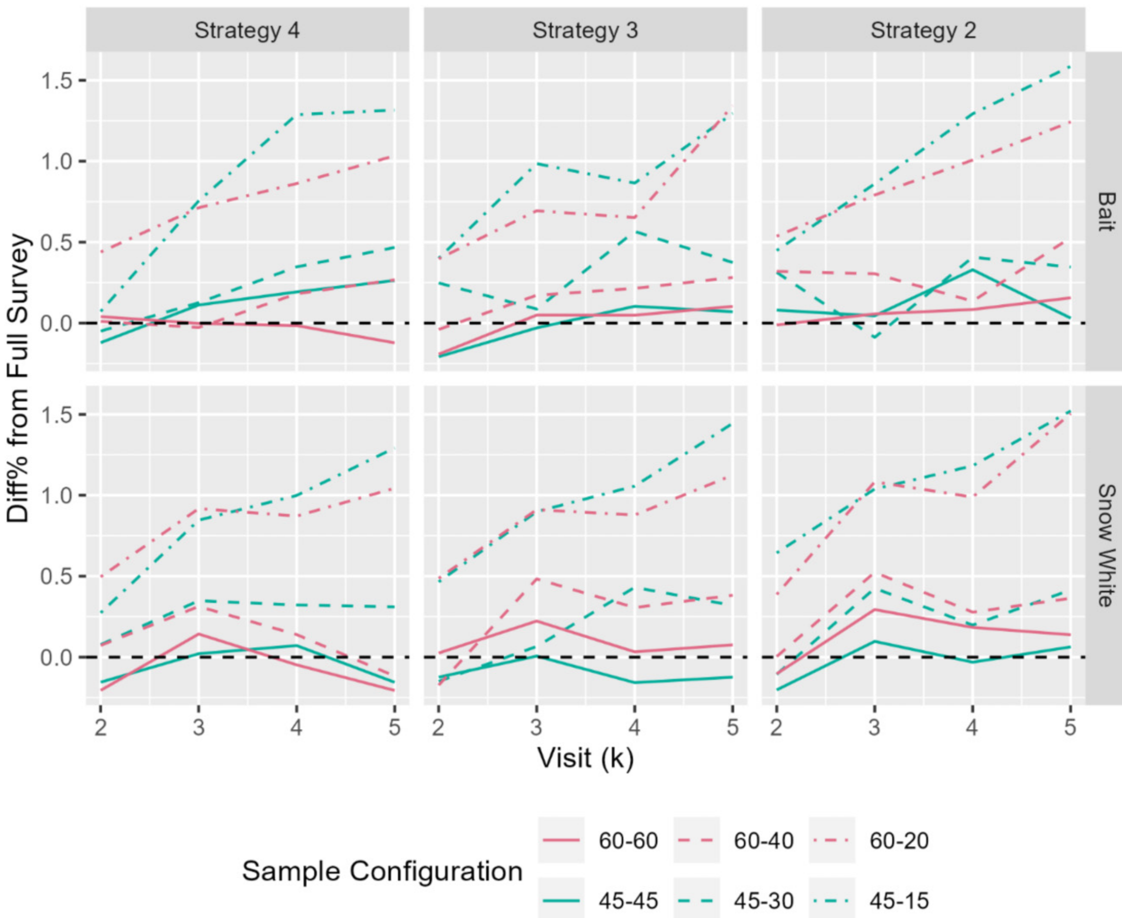

stands had negative temporal trends in the coefficient of variation for volume (Fig. 3). If the coefficient of variation for volume were to increase rather than decrease, it is possible that the relative RMSE of the PUE would increase from that of the first survey, possibly exceeding established maximum error thresholds for VRP surveys, even for cases where $n_1 = n_2$. Our study motivates an understanding of how temporal dynamics of forest stands may affect the coefficient of variation for volume, which can help inform future VRP update methodologies.

In general, the PUE exhibits small biases across all scenarios, with relative absolute biases typically less than 0.5%. We suspect these bias problems, while minor, may follow from the biasedness of double sampling ratio estimators in general (Reich et al. 1993). A typical double sampling ratio estimator (e.g., that used for $\widehat{G}_{2,\mathrm{UE}}$) is only asymptotically unbiased (Singh and Espejo 2007), which implies that a potential bias in the PUE could be exacerbated by small sample sizes. Users of the PUE should be cautious of potential biases, especially for smaller sample sizes that were not covered in our study.

4.2. Variance estimation of the PUE

We proposed a bootstrap estimator for the PUE and assessed its performance under simulation. In general, the bootstrap variance estimator is deflated, with relative bias values as low as −8%. While it is difficult to find studies that apply a bootstrap variance estimator in the same context, some lines can be drawn to other research that may explain this result, especially if we focus our attention on $\widehat{G}_{2,\mathrm{DS}}$, which is a classical application of a double sampling estimator. The study we developed our bootstrap variance estimator from, Schreuder et al. (1987), also found a negative bias in the bootstrap variance estimator when n_2 is small, with relative bias values of −82.9%, −10.5%, and 2.1% across three populations using a sample size of $n_1 = 120$ and $n_2 = 10$. This bias became smaller with larger n_2 sample sizes. Sitter (1997), who further developed the methods from Schreuder et al. also note under coverage of a 90% bootstrap confidence interval for a double sampling regression estimator in some simulation scenarios, ranging between 82.2% and 91.4%, which may imply a deflated variance estimator. They discovered deflated coverage when $\bar{x}' - \bar{x}$ is large but did not

Fig. 7. Relative bias of the product update variance estimator for each sampling design for each stand at each visit obtained from the Monte Carlo simulation. The sampling scenarios are grouped by their strategy, i.e., the approximate number of measure trees per plot selected at the revisit, and their visit, i.e., the temporal index describing the time since the initial survey. Each sampling design code on the X axis refers to the number of field plots collected at the first visit, the number of field plots collected at the second visit, and the approximate number of measure trees selected per plot at the second visit.

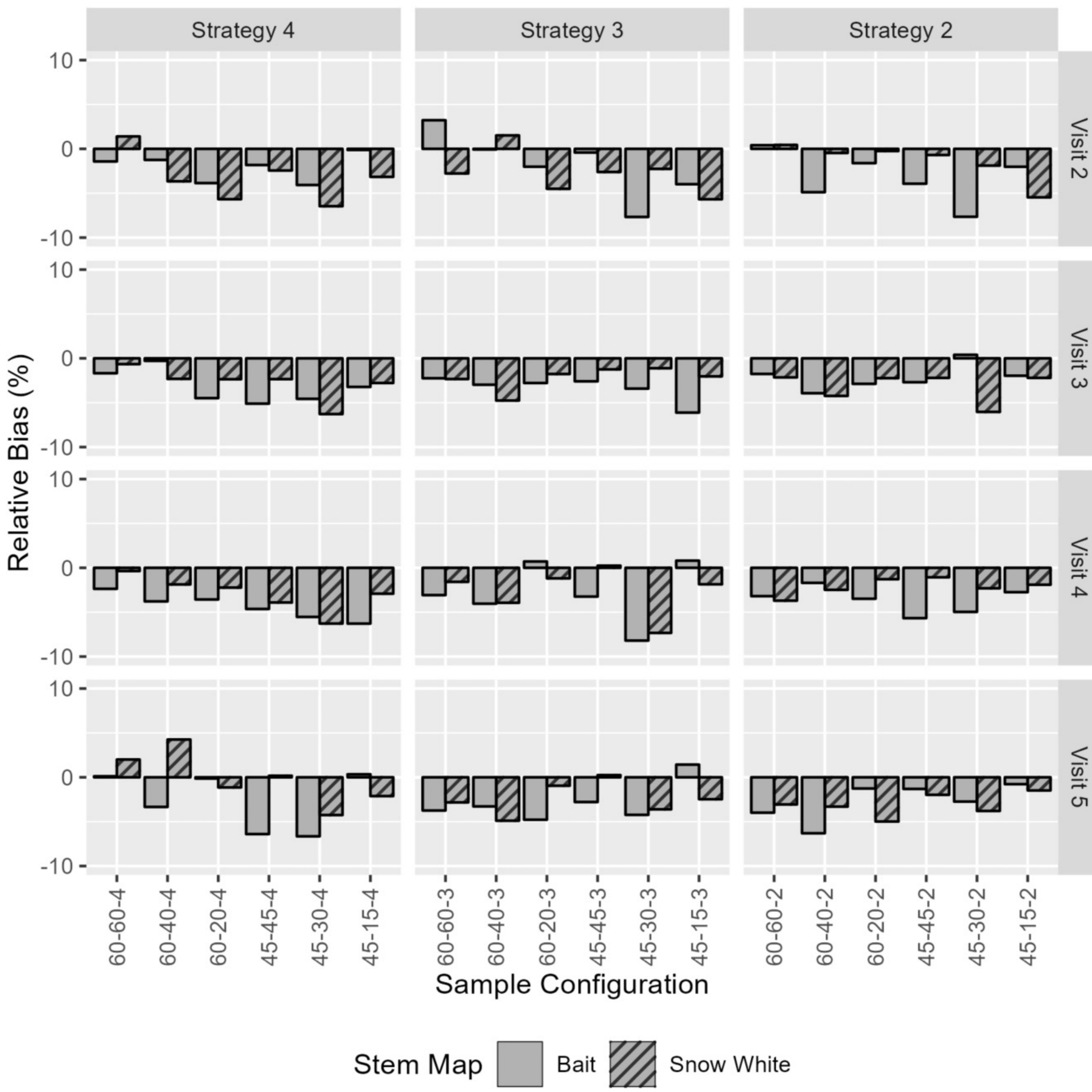

observe the opposite effect when the quantity was small, leading to deflated confidence interval coverage over the set of all samples.

Our bootstrap variance estimator did not randomly select trees with replacement inside of the plot-level measure tree sets. Rather, the only source of randomization in the bootstrap is from sampling with replacement over the plot-level index sets $\mathcal{I}_1$ and $\mathcal{I}_2$ (see Appendix B). In some respects, this approach is similar to what is described as "cluster bootstrapping" (Field and Welsh 2007) if the plot-level measure tree sets are viewed as clusters. Cluster bootstrapping is known to produce deflated variance estimates (Davison and Hinkley 1997; Field and Welsh 2007), which may explain some of the negative bias we observed in our variance estimator. However, for our simulation study, the variance of $\widehat{R}_{2,\mathrm{UE}}$ was relatively small compared to that of $\widehat{G}_{2,\mathrm{UE}}$ and we expect that the largest sources of negative bias in the variance estimator are due to negative biases for the variance of $\widehat{G}_{2,\mathrm{UE}}$, which are unrelated to sampling with replacement over the plot-level measure tree sets.

While the negative bias of the PUE bootstrap variance estimator is apparent, it should be discussed in the context of common practice in VRP surveys, which typically involve two-dimensional systematic sampling of field plots. In these situations, the variance estimator for the PUE will likely inflate, especially when spatial autocorrelation exists in, for example, the plot-level tallies used to estimate G. While it is impossible to say a priori how much a systematic design will inflate the variance estimator, since this relies on the structure of the population under study and the particular systematic design employed by the surveyor (Magnussen et al. 2020; Frank and Monleon 2021), we expect that systematic sampling will at least mitigate some of the negative bias in the PUE variance estimator in practice.

4.3. Practical implementation

The implementation of an updated VRP survey in the field requires some consideration of typical practices when installing an original survey. The PUE requires the surveyor to locate previously installed plots. Permanent plot identifiers, such as field flagging and plastic or metal stakes, along with global navigation satellite system (GNSS) coordinates can facilitate the location of previously installed plots. Importantly, the PUE requires knowledge of whether a tree is remeasured when determining which trees belong to the set of additional trees, $\mathcal{A}_{2i}$, or, conversely, to the set of previously measured trees, $\dot{\mathcal{T}}_{1i}$, at $t = 2$. If trees are physically identified with timber marking paint or tags, then this determination is trivial, but this may not always be the case in practice. In personal communications with VRP surveyors, we found that information from the previous survey is vital for this determination when no permanent tree identifiers exist. This information should include the previously used BAF, previous measurements of diameter, and any information describing how the measure trees were selected, e.g., starting from North and working clockwise (K. Bailey, A. Coleman, personal communication, 2023). The surveyors also felt that large amounts of disturbance, such as windthrow events, stands where the trees are very similar, or stands where visibility is poor due to tall shrubs would make this determination more difficult. If the use of the PUE is anticipated before the first survey is installed, then surveyors should assign a unique physical identifier to each measure tree which increases the reliability of this determination at later visits, which many surveyors already do.

VRP surveys are often concerned with the simultaneous estimation of many variables, including merchantable timber volume disaggregated by species, diameter class, and others (e.g., Bell and Dilworth 2014, p. 234). In this study, we developed the PUE with only one variable in mind, the merchantable timber volume without any level of disaggregation into other subpopulations. The PUE can be readily extended to other variables of interest, much in the same manner that the product estimator can be used to estimate other quantities that are not volume. This involves replacing v_{ijt}, the tree volume at a given time point, with some other variable, e.g., y_{ijt}. Any number of interesting variables can be entertained, such as biomass or carbon calculated from allometric equations (e.g., Hoover et al. 2018). What is unique to the PUE, however, is the subsampling of tally plots used at $t = 2$, and we caution potential users of the PUE that it may be the case that a variable of interest is not captured during the second survey that was observed during the first survey. For example, if the variable of interest for G is the basal area per hectare of some rare species in the stand, then it is possible to observe a value of $\widehat{G}_2 = 0$ if the species is not captured on the second visit, which updates $\widehat{G}_{2,\mathrm{UE}}$ to a value of zero. For these cases, alternative sampling designs could be entertained that would efficiently select revisit plots that consider rare subpopulations, such as double sampling for stratification.

5. Conclusion

We presented an estimator for updating prior VRP surveys. The estimator is the product of two estimators, one that updates the basal area and one that updates the VBAR, called the PUE. We examined the PUE under repeated sampling of two stands from northwest Washington, USA. The PUE demonstrated relative biases ranging between −0.3% and 0.8%. In our simulation study, the PUE achieved smaller relative RMSEs than the initial survey, typically when revisiting two thirds of the initial plots or greater and achieved relative RMSEs within 1% of the initial survey when revisiting just one third of the initial plots, which implies that the PUE reduces the field effort while producing surveys of similar quality when VRP survey updates are necessary. We consider this work a foundational effort for creating the PUE, but many research questions remain, especially with regard to practical approaches for sample size planning when conducting a VRP revisit.

Acknowledgements

We thank the Olympic National Forest for hosting the Olympic Habitat Development Study and implementing the thinning treatments and crews from the Pacific Northwest Research Station for installing the stem mapped stands. Measurements were conducted by crews from the Pacific Northwest Research Station and from J and M Forestry. We thank Matthew Rainey of the Bureau of Land Management for his initial ideas involving VRP updates and advice about practical implementation.

Article information

History dates

Received: 26 February 2024
Accepted: 7 June 2024
Accepted manuscript online: 18 June 2024
Version of record online: 3 October 2024

Copyright

Data availability

Data generated or analyzed during this study are available from the corresponding author upon reasonable request. A sample collected from the Bait stand is provided in the supplemental material.

Author information

Author ORCIDs

Bryce Frank https://orcid.org/0000-0003-2980-6860
Francisco Mauro https://orcid.org/0000-0002-7832-6268

Author contributions

Conceptualization: BF, FM, CAH, KRF
Data curation: BF, CAH
Formal analysis: BF, FM
Methodology: BF, FM, KRF
Writing – original draft: BF
Writing – review & editing: FM, CAH, KRF

Competing interests

The authors declare there are no competing interests.

Funding information

BF and KRF were supported by USDI Bureau of Land Management and USDA Forest Service during the duration of this research. FM was supported by the Maria Zambrano's Excellence Program (#E-42-2022-0000233) from the Ministry of Science and Innovation and funded by the University of Valladolid and European Union-NextGeneration.

Supplementary material

Supplementary data are available with the article at https://doi.org/10.1139/cjfr-2024-0050.

References

American Carbon Registry. 2021. Methodology for the quantification, monitoring, reporting and verification of greenhouse gas emissions reductions and removals from small non-industrial private forestlands. Available from https://acrcarbon.org/wp-content/uploads/2023/03/ACR-IFM-Small-Non-Industrial-v1.0.pdf [accessed 7 November 2023].

Barrett, T.M. 2006. Optimizing efficiency of height modeling for extensive forest inventories. Can. J. For. Res. **36**(9): 2259–2269. doi:10.1139/x06-128.

Bell, J.F., and Dilworth, J.R. 2014. Log scaling and timber cruising. Cascade Printing Company.

Bitterlich, W. 1984. The relascope idea. Relative measurements in forestry. Commonwealth Agricultural Bureaux. Available from https://www.cabdirect.org/cabdirect/abstract/19850699408 [accessed 20 February 2024].

Cochran, W.G. 1977. Sampling techniques. Wiley.

Dahl, C.A., Harding, B.A., and Wiant, H.V., Jr. 2008. Comparing double-sampling efficiency using various estimators with fixed-area and point sampling. North. J. Appl. For. **25**(2): 99–102. doi:10.1093/njaf/25.2.99.

Davison, A.C., and Hinkley, D.V. 1997. Bootstrap methods and their application. Cambridge University Press. doi:10.1017/cbo9780511802843.

Dellenbaugh, M., Ducey, M.J., and Innes, J.C. 2007. Double sampling may improve the efficiency of litterfall estimates. Can. J. For. Res. **37**(4): 840–845. doi:10.1139/X06-274.

Ducey, M.J. 2009. Sampling trees with probability nearly proportional to biomass. For. Ecol. Manag. **258**(9): 2110–2116. doi:10.1016/j.foreco.2009.08.008.

Field, C.A., and Welsh, A.H. 2007. Bootstrapping clustered data. J. R. Stat. Soc. Ser. B Stat. Methodol. **69**(3): 369–390. doi:10.1111/j.1467-9868.2007.00593.x.

Flewelling, J.W., and Strunk, J.L. 2013. The walk through and fro estimator for edge bias avoidance. For. Sci. **59**(2): 223–230. doi:10.5849/forsci.10-135.

Frank, B., and Monleon, V.J. 2021. Comparison of variance estimators for systematic environmental sample surveys: considerations for post-stratified estimation. Forests, **12**(6): 772. doi:10.3390/f12060772.

Hamilton, F., Penny, R., Black, P., Cumming, F., and Irvine, M. 1999. Victoria's statewide forest resource industry—an outline of methods. Aust. For. **62**(4): 353–359. doi:10.1080/00049158.1999.10674803.

Henttonen, H.M., and Kangas, A. 2015. Optimal plot design in a multipurpose forest inventory. For. Ecosyst. **2**(1): 31. doi:10.1186/s40663-015-0055-2.

Hoover, C.M., Ducey, M.J., Colter, R.A., and Yamasaki, M. 2018. Evaluation of alternative approaches for landscape-scale biomass estimation in a mixed-species northern forest. For. Ecol. Manag. **409**: 552–563. doi:10.1016/j.foreco.2017.11.040.

Hou, Z., Mehtätalo, L., McRoberts, R.E., Ståhl, G., Tokola, T., Rana, P., et al. 2019. Remote sensing-assisted data assimilation and simultaneous inference for forest inventory. Remote Sens. Environ. **234**: 111431. doi:10.1016/j.rse.2019.111431.

Hsu, Y.-H., Chen, Y., Yang, T.-R., Kershaw, J.A., and Ducey, M.J. 2020. Sample strategies for bias correction of regional LiDAR-assisted forest inventory estimates on small woodlots. Ann. For. Sci. **77**(3): 75. doi:10.1007/s13595-020-00976-8.

Iles, K. 2012. Some current subsampling techniques in forestry. Math. Comput. For. Nat. Resour. Sci. **4**(2): 77.

Magnussen, S., McRoberts, R.E., Breidenbach, J., Nord-Larsen, T., Ståhl, G., Fehrmann, L., and Schnell, S. 2020. Comparison of estimators of variance for forest inventories with systematic sampling-results from artificial populations. For. Ecosyst. **7**(1): 1–19. doi:10.1186/s40663-020-00223-6.

Marshall, D.D., Iles, K., and Bell, J.F. 2004. Using a large-angle gauge to select trees for measurement in variable plot sampling. Can. J. For. Res. **34**(4): 840–845. doi:10.1139/x03-240.

McRoberts, R.E., Næsset, E., Hou, Z., Ståhl, G., Saarela, S., Esteban, J., et al. 2023. How many bootstrap replications are necessary for estimating remote sensing-assisted, model-based standard errors? Remote Sens. Environ. **288**: 113455. doi:10.1016/j.rse.2023.113455.

Reich, R.M., Bonham, C.D., and Remington, K.K. 1993. Double sampling revisited. J. Range Manage. **46**(1): 88–90.

Roberts, S.D., Harrington, C.A., and Buermeyer, K.R. 2007. Does variable-density thinning increase wind damage in conifer stands on the Olympic Peninsula? West. J. Appl. For. **22**(4): 285–296. doi:10.1093/wjaf/22.4.285.

Särndal, C.-E., Swensson, B., and Wretman, J. 2003. Model assisted survey sampling. Springer Science & Business Media.

Schreuder, H.T., Li, H.G., and Scott, C.T. 1987. Jackknife and bootstrap estimation for sampling with partial replacement. For. Sci. **33**(3): 676–689. doi:10.1093/forestscience/33.3.676.

Scott, C.T., and Köhl, M. 1994. Sampling with partial replacement and stratification. Forest Sci. **40**(1): 30–46. doi:10.1093/forestscience/40.1.30.

Scott, C.T. 1990. An overview of fixed versus variable-radius plots for successive inventories. *In* State-of-the-art methodology of forestry inventory. 30 July - 5 August. Syracuse, NY, USA. Available from https://www.fs.usda.gov/pnw/pubs/pnw_gtr263/pnw_gtr263ac.pdf [accessed 7 November 2023].

Shao, J. 2003. Impact of the bootstrap on sample surveys. Stat. Sci. **18**(2): 191–198. doi:10.1214/ss/1063994974.

Singh, H.P., and Espejo, M.R. 2007. Double sampling ratio-product estimator of a finite population mean in sample surveys. J. Appl. Statist. **34**(1): 71–85. doi:10.1080/02664760600994562.

Sitter, R.R. 1997. Variance estimation for the regression estimator in two-phase sampling. J. Am. Statist. Assoc. **92**(438): 780–787. doi:10.1080/01621459.1997.10474031.

Stewart, B. 2007. Sampling efficiencies of new and existing variable radius plot growth estimators. PhD thesis, University of Georgia. Available from http://getd.libs.uga.edu/pdfs/stewart_brock_t_200712_phd.pdf [accessed 7 November 2023].

USDA Forest Service. 1993. Timber cruising handbook. Available from https://www.fs.usda.gov/Internet/FSE_DOCUMENTS/fsbdev2_029371.pdf [accessed 5 November 2023].

Van Deusen, P.C., and Meerschaert, W.J. 1986. On critical-height sampling. Can. J. For. Res. **16**(6): 1310–1313. doi:10.1139/x86-231.

Wang, Y. 2023. Volume estimator library equations. Available from https://www.fs.usda.gov/forestmanagement/products/measurement/volume/nvel/index.php [accessed 2 February 2024].

Williams, M.S. 2001. Comparison of estimation techniques for a forest inventory in which double sampling for stratification is used. For. Sci. **47**(4): 563–576. doi:10.1093/forestscience/47.4.563.

Wilm, H.G., Costello, D.F., and Klipple, G.E. 1944. Estimating forage yield by the double-sampling method. Agron. J. **36**(3). doi:10.2134/agronj1944.00021962003600030003x.

Yang, H., Magnussen, S., Fehrmann, L., Mundhenk, P., and Kleinn, C. 2016. Two neighborhood-free plot designs for adaptive sampling of forests. Environ. Ecol. Stat. **23**(2): 279–299. doi:10.1007/s10651-015-0339-2.

Appendix A. An approach for constructing feasible subsampling strategies

The product update estimator (PUE) requires the determination of three subsampling rates used to select measure trees at $t = 1$ and $t = 2$. During an initial phase of this study, we noticed that the number of additional measure trees at the $t = 2$, $\dot{A}_2$, could become extremely large, especially when the initial remeasurement rate $p_{\dot{\mathcal{T}}_1}$ is small. To refine the practical implementation of the PUE, we used an approach that assumes the variable radius plot (VRP) surveyor does not wish to exert a measurement effort greater than the effort used for the initial survey for a given VRP sample point (Section 2.4.2). This constraint ensures that the second survey can be done in at most the same time, in the sense of an expected value at a given plot, than the initial survey, provided some prior information about needed parameters are available. Appendix A sketches an approach for constructing feasible subsampling rates by imposing constraints on the expected effort at $t = 2$ using an optimization procedure.

We assume that the measurement effort is quantified by the number of measure trees collected by the surveyor, which is expressed as a plot-level expectation. We obtain the efforts

$$e_1 = E\left(\dot{T}_{1i}\right) \tag{A1}$$

$$e_2 = E\left(\ddot{T}_{1i} + \dot{A}_{2i}\right) \tag{A2}$$

For the $t = 1$ effort we obtain

$$E\left(\dot{T}_{1i}\right) = \frac{G_1}{F} p_{\dot{\mathcal{T}}_1} = e_1 \tag{A3}$$

where F is the basal area factor. For the first term of the $t = 2$ effort we obtain

$$E\left(\ddot{T}_{1i}\right) = \frac{G_1 - G_M}{F} p_{\dot{\mathcal{T}}_1} p_{\ddot{\mathcal{T}}_1} \tag{A4}$$

where G_M is the basal area mortality that occurred between visits, which assumes that mortality trees are not measured as part of $t = 2$. For the second term of the $t = 2$ effort begin by noting

$$E\left(A_{2i}\right) = E\left(T_{2i} - \left(\dot{T}_{1i} - \dot{M}_{1i}\right)\right) \tag{A5}$$

which is the expected value of the size of the additional tree set. The term $\dot{T}_{1i} - \dot{M}_{1i}$ quantifies the number of trees eligible for remeasurement at $t = 2$, and $\dot{M}_{1i}$ is the number of initially measured trees that experienced mortality, which are not included in T_{2i} and thus need to be subtracted from the initial measure trees. Applying the expectation, we obtain

$$E\left(A_{2i}\right) = \frac{G_2}{F} - \left(\frac{G_1}{F} - \frac{G_M}{F}\right) p_{\dot{\mathcal{T}}_1} \tag{A6}$$

Noting that $E\left(\dot{A}_{2i}\right) = E\left(A_{2i}\right) p_{\dot{\mathcal{A}}_2}$ we obtain

$$E\left(\dot{A}_{2i}\right) = \frac{G_2}{F} p_{\dot{\mathcal{A}}_2} - \left(\frac{G_1}{F} - \frac{G_M}{F}\right) p_{\dot{\mathcal{T}}_1} p_{\dot{\mathcal{A}}_2} \tag{A7}$$

Finally, we obtain the expected effort at $t = 2$

$$E\left(\ddot{T}_{1i} + \dot{A}_{2i}\right) = \frac{G_1 - G_M}{F} p_{\dot{\mathcal{T}}_1} \left(p_{\ddot{\mathcal{T}}_1} - p_{\dot{\mathcal{A}}_2}\right) + \frac{G_2}{F} p_{\dot{\mathcal{A}}_2} = e_2 \tag{A8}$$

With the $t = 1$ and $t = 2$ efforts quantified, we proceed toward constructing an optimization to determine the sampling rates. To begin, we desired an approximately even mixture of additional trees and remeasured trees obtained at $t = 2$. For this we impose the constraints

$$0.9 \leq \frac{E\left(\ddot{T}_{1i}\right)}{E\left(\dot{A}_{2i}\right)} \leq 1.1 \tag{A9}$$

We also wished to ensure that all selection probabilities are nonzero, otherwise both subpopulations of trees will not have representation in the PUE. Therefore, we impose the additional constraints that $p_{\ddot{\mathcal{T}}_1} \geq 0.1$ and $p_{\dot{\mathcal{A}}_2} \geq 0.1$. Finally, the optimization minimizes the objective function

$$f\left(e_2, \tilde{e}_2\right) = \left|e_2 - \tilde{e}_2\right| \tag{A10}$$

where $\tilde{e}_2$ is the desired effort at $t = 2$, i.e., the desired number of plot-level measure trees.

We conducted the optimization by using a grid search procedure. A two-dimensional grid of values for $p_{\ddot{\mathcal{T}}_1}$ and $p_{\dot{\mathcal{A}}_2}$ was generated using steps of size 0.01 on the interval [0, 1]. Values for the objective function and constraints were calculated directly from the stands. Then, the solution that minimized the objective function for each stand, visit and desired effort configuration was selected as the final set of sampling rates. In practice, prior information about the $t = 1$ and $t = 2$ basal areas and basal area mortality can be used to construct candidate sampling rates, much in the same way prior information is used to inform single date VRP survey designs (Marshall et al. 2004; Bell and Dilworth 2014). We highlight that our procedure does not consider optimal sampling strategies with respect to, e.g., the minimization of sampling variance of $\widehat{R}_{2,\mathrm{UE}}$, and we leave such a question for further research.

After applying the optimization procedure, the selected sampling rates can be inspected. Table A1 displays the selected sampling rates for the stands. Only minor discrepancies between the realized and desired effort are apparent, with a maximum absolute deviation of 0.01. In general, both sampling rates decline with the desired effort. $p_{\dot{\mathcal{A}}_2}$ tends to be larger for early visits, likely due to the small temporal lag, which results in less growth than the other visits, and thus

Table A1. Outputs of the sampling rate optimization procedure for each stand, visit, and strategy.

Stand	Visit	Strategy	Realized effort—e_2	$p_{\ddot{\mathcal{T}}_1}$	$p_{\dot{\mathcal{A}}_2}$
Bait	2	4	4.00	0.52	0.56
		3	3.00	0.39	0.42
		2	2.00	0.26	0.28
	3	4	4.00	0.49	0.49
		3	3.02	0.39	0.35
		2	2.00	0.24	0.25
	4	4	4.00	0.52	0.40
		3	3.00	0.39	0.30
		2	2.00	0.26	0.20
	5	4	4.00	0.51	0.35
		3	2.99	0.37	0.27
		2	1.99	0.26	0.17
Snow White	2	4	4.00	0.50	0.72
		3	3.00	0.39	0.52
		2	2.00	0.25	0.36
	3	4	4.00	0.52	0.59
		3	3.00	0.36	0.48
		2	2.00	0.24	0.32
	4	4	4.00	0.48	0.54
		3	2.99	0.39	0.37
		2	2.00	0.24	0.27
	5	4	4.00	0.49	0.46
		3	2.99	0.36	0.35
		2	2.02	0.26	0.22

a smaller pool of $\mathcal{A}_2$ trees. In contrast, $p_{\ddot{\mathcal{T}}_1}$ remains relatively static within a strategy across visits.

Appendix B. Data generating mechanism for bootstrap variance estimator

Appendix B describes the data generating mechanism used to create bootstrap samples for the purposes of variance estimation (Section 2.3). The data generating mechanism largely follows that of Schreuder et al. (1987) for the specific case where $n_2 \le n_1$. Furthermore, the data generating mechanism samples with replacement only over the set of plot-level indices, and does not sample within the tree-level sets for a given plot. Using the first plot as an example, the sets $\dot{\mathcal{T}}_{11}$, $\ddot{\mathcal{T}}_{11}$, and $\dot{\mathcal{A}}_{21}$ are invariant under the bootstrap. In this sense, our approach is similar to that of "cluster bootstrapping", discussed in Field and Welsh (2007) for the special case of equally sized clusters, which selects clusters randomly with replacement but does not select randomly with replacement within a given cluster. See Section 4.2 for further discussion.

The data generating mechanism begins by partitioning the plot-level indices from $t = 1$, $\mathcal{I}_1 = \{1, \ldots, n_1\}$. Refer to the set of revisited plot indices as $\mathcal{I}_2$ and the set of nonrevisited plot indices as $\mathcal{I}_{2-}$ such that $\mathcal{I}_1 = \mathcal{I}_2 \cup \mathcal{I}_{2-}$. For both partitions $\mathcal{I}_2$ and $\mathcal{I}_{2-}$, resample with replacement within each partition using the sample sizes n_2 and $n_1 - n_2$, respectively. For each partition this creates the bootstrapped plot-level indices, $\mathcal{I}_{2,b}$ and $\mathcal{I}_{2-,b}$, respectively and $\mathcal{I}_{1,b} = \mathcal{I}_{2,b} \cup \mathcal{I}_{2-,b}$. Note that:

1. $\mathcal{I}_{1,b}$, $\mathcal{I}_{2,b}$, and $\mathcal{I}_{2-,b}$ are multisets, i.e., they include repeated elements following from simple random sampling with replacement. For bootstrap samples, when calculating components of $\widehat{V}_{\text{PUE,b}}$ that involve sums over these multisets, $\sum_{i \in \mathcal{I}_{1,b}} x_i$ indicates the summation for all elements, including the repeats.
2. The sizes of the tree sets, e.g., $\dot{\mathcal{T}}_1$, can change with each bootstrap iteration, because each bootstrap sample contains a randomly selected set of plots composed of varying numbers of trees. For this purpose, we reserve the nonscripted capital letters to refer to the number of trees in each set and add a b subscript to refer to the bootstrap iteration. For example, $\dot{T}_{1,b}$ refers to the number of measure trees collected at $t = 1$ contained in the bth bootstrap iteration.

We begin by defining each of the bootstrapped component estimators. First, we obtain the bootstrapped estimate of the basal area

$$\text{(B1)} \quad \widehat{G}_{2,\text{UE,b}} = \widehat{G}'_{1,b} \cdot \frac{\widehat{G}_{2,b}}{\widehat{G}_{1,b}}$$

where

$$\text{(B2)} \quad \widehat{G}'_{1,b} = \left(\frac{F}{n_1} \sum_{i \in \mathcal{I}_{1,b}} T_{1i} \right)$$

 Can. J. For. Res. 54: 1213–1229 (2024) | dx.doi.org/10.1139/cjfr-2024-0050

$$\text{(B3)}\quad \widehat{G}_{2,b} = \left(\frac{F}{n_2}\sum_{i\in\mathcal{I}_{2,b}} T_{2i}\right)$$

and

$$\text{(B4)}\quad \widehat{G}_{1,b} = \left(\frac{F}{n_2}\sum_{i\in\mathcal{I}_{2,b}} T_{1i}\right)$$

Next, we obtain the bootstrapped estimate of the VBAR

$$\text{(B5)}\quad \widehat{R}_{2,\mathrm{UE,b}} = \widehat{R}'_{1,b}\cdot\frac{\widehat{R}_{2,b}}{\widehat{R}_{1,b}}$$

Beginning with the VBAR estimate constructed at $t = 1$ we obtain

$$\text{(B6)}\quad \widehat{R}'_{1,b} = \frac{1}{\dot{T}_{1,b}}\sum_{i\in\mathcal{I}_{1,b}}\sum_{j\in\dot{\mathcal{T}}_{1i}}\frac{v_{ij1}}{g_{ij1}}$$

Next, we turn to the update estimator for VBAR

$$\text{(B7)}\quad \widehat{R}_{2,b} = w_{\mathcal{A}_2,b}\widehat{R}_{\dot{\mathcal{A}}_2,b} + w_{\dot{\mathcal{T}}_1,b}\widehat{R}_{\ddot{\mathcal{T}}_1,b}$$

where $w_{\mathcal{A}_2,b} = \frac{A_{2,b}}{T_{2,b}}$ and $w_{\dot{\mathcal{T}}_1,b} = 1 - w_{\mathcal{A}_2,b}$. We obtain the two VBAR estimators at $t = 2$

$$\text{(B8)}\quad \widehat{R}_{\dot{\mathcal{A}}_2,b} = \frac{1}{\dot{A}_{2,b}}\sum_{i\in\mathcal{I}_{2,b}}\sum_{j\in\dot{\mathcal{A}}_{2i}}\frac{v_{ij2}}{g_{ij2}}$$

$$\text{(B9)}\quad \widehat{R}_{\ddot{\mathcal{T}}_1,b} = \frac{1}{\ddot{T}_{1,b}}\sum_{i\in\mathcal{I}_{2,b}}\sum_{j\in\ddot{\mathcal{T}}_{1i}}\frac{v_{ij2}}{g_{ij2}}$$

We obtain the bootstrap estimate of the VBAR obtained using only revisited plots

$$\text{(B10)}\quad \widehat{R}_{1,b} = \frac{1}{\dot{T}_{1,\mathcal{I}_{2,b}}}\sum_{i\in\mathcal{I}_{2}}\sum_{j\in\dot{\mathcal{T}}_{1i}}\frac{v_{ij1}}{g_{ij1}}$$

The bootstrapped component estimators are used to form the bootstrapped PUE. We obtain

$$\text{(B11)}\quad \widehat{V}_{\mathrm{PUE},b} = \left[\widehat{R}'_{1,b}\cdot\frac{\widehat{R}_{2,b}}{\widehat{R}_{1,b}}\right]\cdot\left[\widehat{G}'_{1,b}\cdot\frac{\widehat{G}_{2,b}}{\widehat{G}_{1,b}}\right]$$

Finally, in some bootstrap iterations it may be impossible to construct $\widehat{R}_{1,b}$, $\widehat{R}'_{1,b}$, or $\widehat{R}_{2,b}$. For example, if all plots within a bootstrap iteration are completely devoid of measure trees, then some of the set sizes $\dot{T}_{1,b}$, $\ddot{T}_{1,b}$, or $\dot{A}_{2,b}$ may be zero. In these cases, we discard the bootstrap iteration.